BIOINFORMATICS

Vol. 20 no. 7 2004, pages 1129–1137
DOI: 10.1093/bioinformatics/bth050

CompuCell, a multi-model framework for simulation of morphogenesis

J. A. Izaguirre[1,*], R. Chaturvedi[1], C. Huang[1], T. Cickovski[1], J. Coffland[1], G. Thomas[2], G. Forgacs[3], M. Alber[4], G. Hentschel[5], S. A. Newman[6] and J. A. Glazier[7]

[1]Department of Computer Science and Engineering, [2]Department of Physics, University of Notre Dame, Notre Dame, IN 46556, USA, [3]Department of Physics and Biology, University of Missouri, Columbia, MO 65211, USA, [4]Department of Mathematics, University of Notre Dame, Notre Dame, IN 46556, USA, [5]Department of Physics, Emory University, Atlanta, GA 30332, USA, [6]Department of Cell Biology and Anatomy, New York Medical College, Valhalla, NY 10595, USA and [7]Departments of Physics and Biology and Biocomplexity Institute, Indiana University, Bloomington, IN 47405, USA

Received on March 12, 2003; revised on August 5, 2003; accepted on August 29, 2003
Advance Access publication February 5, 2004

ABSTRACT

Motivation: CompuCell is a multi-model software framework for simulation of the development of multicellular organisms known as morphogenesis. It models the interaction of the gene regulatory network with generic cellular mechanisms, such as cell adhesion, division, haptotaxis and chemotaxis. A combination of a state automaton with stochastic local rules and a set of differential equations, including subcellular ordinary differential equations and extracellular reaction–diffusion partial differential equations, model gene regulation. This automaton in turn controls the differentiation of the cells, and cell–cell and cell–extracellular matrix interactions that give rise to cell rearrangements and pattern formation, e.g. mesenchymal condensation. The cellular Potts model, a stochastic model that accurately reproduces cell movement and rearrangement, models cell dynamics. All these models couple in a controllable way, resulting in a powerful and flexible computational environment for morphogenesis, which allows for simultaneous incorporation of growth and spatial patterning.

Results: We use CompuCell to simulate the formation of the skeletal architecture in the avian limb bud.

Availability: Binaries and source code for Microsoft Windows, Linux and Solaris are available for download from http://sourceforge.net/projects/compucell/

Contact: compucell@cse.nd.edu

1 INTRODUCTION

Our long-term goal is to simulate morphogenesis starting from experimental measurements of gene regulatory networks, cell and extracellular matrix (ECM) properties, and cell–cell and cell–microenvironment interactions. Since genes and their products determine the physical properties of tissues during morphogenesis (Newman and Comper, 1990), useful computational models of multicellular development must describe, in addition to differential regulation of gene activity, cell behaviors such as release of diffusible factors, adhesion and motility (Marée and Hogeweg, 2001).

CompuCell, provides such a computational framework. Independent software modules simulate the interaction of the gene regulatory network with cellular mechanisms; including coupling between biosynthesis and diffusion of morphogens (molecules released by cells that affect the behavior of other cells during development), cell adhesion, haptotaxis (movement of cells along a gradient of a molecule deposited on a substrate) and chemotaxis (movement of cells along a gradient of a chemical diffusing in the extracellular environment). The three main components of CompuCell are the cellular Potts model (CPM) that describes cell and ECM behaviors, a Reaction–Diffusion (RD) module that describes diffusible morphogens and a combined ODE/state model of genetic regulatory networks and differentiation. We presented an early version of CompuCell in Chaturvedi *et al.* (2003).

The literature on modeling morphogenesis is extensive. Held (2002) provides a good summary. Most current models for morphogenesis are based on purely continuum approaches or discrete cellular automata. CompuCell uses a combination of the two.

Dillon and Othmer (1999) presented a purely continuum model of early limb development. Here, reaction–advection–diffusion between two organizing regions produces the shape of the growing limb in two dimensions (2D). The Navier–Stokes equations model growth. Disadvantages of this

*To whom correspondence should be addressed.

approach are the complex implementation required to handle the moving boundary when solving the PDEs and instabilities due to the advective term. Maini and coworkers have used the moving finite element method to solve similar problems, discussed, e.g. example, in Page *et al.* (2001).

Marée (2000) among others has used cellular automata like the CPM to model the development of *Dictyostelium discoideum.* Recently, Merks *et al.* (2003) have used a combination of lattice-gas automata, advection–diffusion and a discrete model of branching to model coral reef growth. These studies validate the CPM approach that we use in COMPUCELL. Work by Upadhyaya (2000) also contains data validating the CPM.

We use the CPM to model cell dynamics. Continuum models of cells are also available. For example, Drury and Dembo (2001) have used a continuum model with a finite element discretization to model human neutrophils.

COMPUCELL can model a genetic regulatory network of arbitrary complexity. Data on such networks are available in studies that focus on the biochemical reactions inside individual cells. Arkin *et al.* (1998) and McAdams and Arkin (1999) have modeled genetic regulatory and metabolic networks in detail. They analyze the network of metabolic and genetic reactions governing cellular development and apply principles of control systems to predict cell behavior and differentiation in response to internal and external signals. Simulations taking such models into account would be a fruitful extension of the present work.

We illustrate the COMPUCELL framework by simulating the formation of skeletal architecture in the avian limb bud, a classical model of tissue growth, differentiation and patterning.

2 SYSTEMS AND METHODS

2.1 The CPM: cell and tissue growth and movement

We model tissue growth and movement using the CPM (Graner and Glazier, 1992). The CPM has two specific features that differ from most other models of cellular dynamics. It is a cell level model, describing individual generalized cells (which may be real cells, ECM, medium, etc.) as spatially extended objects. Hence, it is potentially more accurate than continuum models or models which treat cells as point particles. It incorporates phenomenologically observed cell behaviors using mathematical constraints, and expressing these constraints as terms in the overall effective energy of the tissue, E. From a mathematical point of view, we can portray any repeatable behavior of a cell in the form of a response consistent with a constraint. Divergence from the correct response exacts an 'energy penalty'. The chosen dynamics reduces the penalty, gradually relaxing the pattern to one consistent with the constraint. While the representation of phenomena like chemotaxis, cell polarity or mitosis as constraints is non-obvious, the method has the great advantage that we can introduce additional mechanisms into the model in a straightforward manner by adding additional constraints.

The original CPM drew on the differential adhesion hypothesis (Steinberg, 1998) to quantitatively reproduce cell movement and rearrangement based on the minimization of cell–cell surface interaction energy (Mombach *et al.*, 1995). Our extended model includes terms that provide for the haptotactic or chemotactic response of cells to gradients of soluble or bound morphogens in the extracellular space.

The CPM is easier to implement, though somewhat slower, than continuum models. For example, consider reaction–advection–diffusion of morphogens in the extracellular space. Implementing advection with continuum models has numerical pitfalls. If we model motions of cells, intracellular medium and ECM using the CPM, we have to deal only with reaction and/or diffusion of morphogens when discretizing the partial differential equations. Theoretically, we can even model reaction and diffusion using cellular automata like the CPM.

The CPM minimizes the effective energy E in the dissipative limit according to Metropolis Monte Carlo dynamics. Cells rearrange into thermodynamically favorable configurations. One weakness of the CPM is that dissipation results from the dynamics and is not introduced explicitly.

We implement the CPM by superimposing a lattice on the cells. Each lattice site (also called a pixel) has an associated index (also called a spin in the literature). The value of the index at a lattice site is σ if the site lies in cell σ. All sites with index σ theoretically belong to the same cell. The probability that all such sites connect is high since disconnected domains induce an energy penalty, cf. Equations (1) and (2).

We describe the net interaction between two cell membranes by a binding energy per unit area, $J_{\tau,\tau'}$. Here τ, τ' are the types of the cells on either end of the link connecting sites with dissimilar indices. The contact energy is thus:

$$E_{\text{Contact}} = \sum_{\text{pixels}\sigma,\sigma'\text{adjacent}} J_{\tau(\sigma),\tau(\sigma')}. \qquad (1)$$

While the absolute values of $J_{\tau,\tau'}$ do not change the equilibrium configurations, the relative strength of the bonds does. The choice of the zero-point of the energy, however, does have subtle effects, e.g. on diffusion constants (Upadhyaya, 2000), which are not relevant to our simple example.

At any time t, a 2D cell of type τ has a surface area $s(\sigma,\tau)$. Equation (2) penalizes a cell's variation in s from its target value.

$$E_{\text{area}} = \sum_{\text{all-cells}} \lambda[s(\sigma,t) - s_{\text{target}}(\sigma,t)]^2. \qquad (2)$$

An additional constraint can regulate cell perimeter. In 3D, corresponding terms can be written for volume and surface area.

To model the growth of a cell, a separate sub-model governs the increase of $s_{\text{target}}(\sigma, \tau)$ with time. To incorporate cell division we start with a cell of average size and let it grow until it doubles in size, at which point we split the cell into two daughters. We assign each daughter cell a unique spin σ. We can model cell death by setting $s_{\text{target}}(\sigma, \tau)$ in Equation (2) to zero.

Chemotaxis or haptotaxis requires additional fields to describe the concentrations $C(\vec{x})$ of the signaling molecules. The equations for the evolution of these fields depend on the particular molecule. The CPM formalism models the chemotactic or haptotactic response of cells by introducing an effective chemical energy, E_{Chemical}, with effective chemical potential $\mu(\sigma)$, resulting in the cell executing a biased motion along the gradient of $C(\vec{x})$.

$$E_{\text{Chemical}} = \mu(\sigma) C(\vec{x}). \tag{3}$$

Again, Equation (3) represents a significant simplification of the biology. It assumes that the velocity of the cell in response to a gradient is independent of the concentration and that the cell does not adapt to external stimuli. We can incorporate such phenomena by making $\mu(\sigma)$ time dependent and including more complex dependences on C and its gradient.

In the model, an effective temperature T drives cell membrane fluctuations. If a proposed change in configuration (i.e. change in the spins associated with sites of the lattice) produces a variation in effective energy, ΔE, we accept it with probability:

$$P(\Delta E) = \min(1, \mathrm{e}^{-\Delta E/kT}), \tag{4}$$

where k is a constant converting T into units of energy. Again, this form represents a simplification of the biology. Cells move due to complex mechanical structures, e.g. a leading edge. These may show fluctuations with non-Boltzmann spectra and long time correlations. We could introduce such behaviors explicitly by changing the functional form of Equation (4) or by using explicit constraints that take into account these correlations. We can also incorporate dissipative effects due to the mechanical rigidity of the cells or ECM into Equation (4). Marée (2000) and Glazier and Graner (1993) contain suggestions on how to choose parameters for the CPM.

2.2 Pattern formation

We use a system of reaction–diffusion PDEs to model the spatial patterning of morphogens (Turing, 1952; Meinhardt and Gierer, 2000; Newman and Frisch, 1979). For further discussion of other models of pattern formation see Gilbert (1997).

2.3 Cell differentiation

Cells may respond to morphogens produced by them or their neighbors produce by altering their genetic activity in continuous or discontinuous (switch-like) fashion. Such nonlinear feedback loops can lead to differentiation of cells. We consider that the network of expressed genes and their products embodies a set of rules for cells that governs their growth, division, secretion of morphogens and strength of adhesion. These rules depend on the state of several chemical fields at the intra- and inter-cellular level that we model by differential equations applying them in the appropriate spatial domains. Our formalism specifies alternative cell types and rules that govern transitions between them. This model of gene regulation captures formal, qualitative aspects of regulatory interactions and allows fitting to outcomes of quantitative experiments. Other approaches to modeling gene regulatory networks are possible (e.g. Arkin *et al.*, 1998; Jong, 2002).

3 SOFTWARE

CompuCell is an open-source object-oriented framework available in Source Forge (http://sourceforge.net/projects/compucell/). It has the following components: (i) base classes describing the main abstractions of morphogenesis, namely cells, chemical fields and spatial/temporal domains; (ii) energy functions and algorithms for the CPM simulation model; (iii) RD and diffusion solvers, including finite difference and finite element discretizations; (iv) cell differentiation models, including an ODE solver and cell type automata; (v) a cross-platform GUI based on the Fox toolkit (http://www.fox-toolkit.org/); (vi) an XML-based front-end (http://xml.apache.org/xerces-c/index.html); and (vii) VTK (http://public.kitware.com/VTK/get-software.php), OpenGL (http://www.opengl.org/) or VRML (http://www.vrmlsite.com/) visualization toolkits, with support for Phantom haptic interfaces (http://www.sensable.com/).

We specify the computational model using XML configuration files containing simulation parameters and their values in pairs, a visualization file (optional), and a Potts initial file to allow an arbitrary initial cell distribution. Optionally, CompuCell can initialize the cell distribution in the lattice to be uniform or random.

Each CompuCell simulation requires a cell model declaration. Cell models describe one or more cell differentiation types and the state variables associated with each cell type. We can define additional differentiation events such as Algorithm (4).

The overall algorithm is Algorithm (1). Each step of the CPM consists of Algorithms (2) and (3). The cell differentiation step is user-defined. In our example, it takes the form of Algorithm (4).

3.1 Performance data

Table 1 presents data for a Sun Blade 1000 with a 900 MHz CPU and 512 MB of memory. For the same grid size, the number of cells does not much affect the speed. Thus, the algorithms scale for quantities dependent on the number of cells.

Algorithm 1: Main loop of COMPUCELL

For total number of combined steps do
  Solve RD (Equation (5))
  Solve N steps of the CPM (Algorithm 2)
  Solve cell state ODEs
  Do cell differentiation
  Grow domains for RD and CPM
end

Algorithm 2: Cellular Potts model

For number of grid points in Potts lattice do
  Compute E_{old} according to Equations (1)–(3)
  Attempt substitution of random pixel by a neighbor
  Compute E_{new} according to Equations (1)–(3)
  Apply Metropolis criterion, Equation (4)
  If cell is growing, attempt division (Algorithm 3)
end

Algorithm 3: Cell division

Breadth-first search do
  Start from selected cell boundary pixel
  Keep track of visited pixels
  Keep track of neighbors awaiting processing
  Ignore pixels outside dividing cell
end
If S_{target} pixels are in list of visited pixels then
  rename them as a new cell

Algorithm 4: Example of cell differentiation

If cell type is non condensing
  and activator concentration > threshold then
    cell type := condensing
    haptotaxis to SAM := on
    SAM production := on
end

Table 1. Runtimes for different grid sizes and numbers of cells on a Sun Blade 1000 with a 900 MHz CPU and 512 MB of memory

Grid Size	Number of cells	Cell density (%)	Total iterations	Simulation (visualization excluded) time (min)
150 × 150	100	64	700	2.5
300 × 300	900	64	700	6
600 × 600	900	64	700	18
150 × 150	325	52	700	3.5

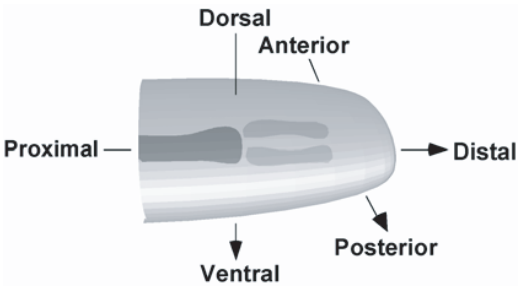

Fig. 1. Schematic representation of a developing vertebrate limb: The three major axes are indicated, as are the first two tiers of skeletal elements to form. In the chicken forelimb these are the humerus, shown as already differentiated (dark gray), followed by the radius and ulna, which are in the process of forming (light gray). Still to form are the wrist bones and digits. The apical ectodermal ridge runs along the distal tip of the limb approximately between the two points intersected by the arrow indicating the AP axis.

4 EXAMPLE: LIMB DEVELOPMENT

In this section, we discuss the biology of skeletal patterning in chick limb and the specific assumptions and simplifications we make in our COMPUCELL simulation.

Our 2D simulation of chick limb morphogenesis generates the arrangement of bones in a forelimb, viewed palm down on a flat surface. In Figure 1 the long axis is proximodistal (PD). The anteroposterior (AP) direction runs from thumb to little finger. The dorsoventral (DV) direction traverses the limb from the back to front. Because the number of elements along the dorsoventral axis does not change during normal development of the vertebrate limb (it always remains one skeletal element in thickness), a 2D representation captures the key patterns seen in Figure 1. However, asymmetry along the dorsoventral axis is important for the functioning of the limb. A complete model of limb development must eventually include all three dimensions.

In the chicken, as in all vertebrates, skeletal pattern formation occurs within tissue surrounded by a thin bounding layer of ectoderm. We neglect this separate structure in these initial simulations. However, the apical ectodermal ridge (AER), a narrow strip of ectoderm running along the apex (distal boundary) of the growing limb bud in the anteroposterior direction, is necessary for elongation and patterning of the limb, and is part of the model. The AER releases fibroblast growth factors (FGFs) which control cell division and production of other morphogens.

Experiments suggest that in limb growth and patterning, the space within the developing limb consists of three zones—an apical zone where only growth takes place, an *active zone* in which cells rearrange locally into precartilage condensations and a frozen zone in which condensations have progressed to differentiated cartilage and no additional patterning takes place. Later, bone replaces the cartilaginous skeleton isomorphically in species with a bony skeleton. Growth continues

in both active and frozen zones. The exact definitions and nature of these zones are still being debated (Dudley *et al.*, 2002; Saunders, 2002; Wolpert, 2002). Each zone has distinct dynamics governing the evolution of cells and of morphogens in the extracellular space. The zones themselves grow and their interfaces move distally.

Both experiment and theory suggest that in the active zone one or more members of the TGF-β family of growth factors acts as an activating RD morphogen (Newman, 1988; Newman *et al.*, 1988; Leonard *et al.*, 1991). We also assume, following recent experiments (Moftah *et al.*, 2002), that sites of incipient condensation release a laterally inhibitory morphogen, a necessary component of most RD schemes (Meinhardt and Gierer, 2000).

Dillon and Othmer (1999) proposed that reaction–advection–diffusion of a growth factor produced in the AER and the morphogen Sonic Hedgehog produced in the zone of polarizing activity (ZPA) at the posterior margin of the bud shape the early limb bud. The ZPA influences the shaping of limb bud and the AP identity of the cells. Wolpert (2002) proposed 'progress zone' and 'positional information' models in which the number of divisions a cell undergoes while in the apical zone controls differentiation of cells in the PD direction, and a chemical gradient with its source at the ZPA provides the cells with information of AP identity.

CompuCell can simulate these as well as other models. In our example, we assume that cell division is uniform throughout all zones of the limb bud (cf. Lewis, 1975; Bowen *et al.*, 1989). New cells form by division, replenishing the active zone as the limb bud grows. As more and more cells condense into a bonelike pattern, the proximal frozen zone grows as well.

In our model, spatiotemporal patterns of the activating morphogen, established as a result of RD, induce a corresponding set of cell condensations as follows: cells that sense a threshold level of the signal produce and secrete an adhesive substratum and also increase their adhesion to one another. In the actual limb, TGF-β induces cells in the active zone to produce the ECM glycoprotein fibronectin. Fibronectin adheres to the cell surface and causes cells to accumulate at focal sites (Frenz *et al.*, 1989a,b). Cells at these sites also produce the cell-surface adhesion protein N-cadherin, causing them to adhere more strongly to each other (Oberlender and Tuan, 1994). We call the secreted substrate adhesion molecule that promotes haptotaxis SAM, and the cell–cell adhesion molecule CAM. For simplicity, we do not include the feedback of the cells on the morphogen fields due to absorption, secretion and changes in cell boundaries.

4.1 Mathematical model

Our mathematical model of limb bud growth and pattern formation includes the following submodels. Table 2 gives values for the parameters in these equations.

Table 2. Parameter values for the chicken limb simulation

Parameter	Value
$J_{\text{cell,cell}}$	$J_{\text{condensing,condensing}} = 0.5$ $J_{\text{non\_condensing,any\_cell}} = 7.0$ $J_{\text{medium,any\_cell}} = 0.2$
λ	3
S_{target}, in the absence of cell growth	16
μ, for cells in condensing state	25
SAM production rate	0.005 units/step
T	7.0
a	0.017
b	1.015
d	7.1
Grid for RD	100 by 300, $\Delta x = \Delta y = 0.01$, $\Delta t = 2E-6$
$\gamma(y)$	80, if $y < 100$ 200, if $y < 200$ 800, otherwise
Ratio of domain growth for RD : Potts	1 : 1
Ratio of iterations of CPM : RD in a compute cycle	1 : 5.0
'Mitosis doubling time' (growth rate for growing cells)	85 Monte Carlo iterations for the cell volume to double
Target cell density	60%

(1) Condensation of cells due to differential adhesion, growth and division of cells and cell haptotaxis in response to SAM using the CPM (Sections 2.1 and 2.3). For our sample simulation, initially all cells in the active zone are mitosing and not condensing (i.e. dividing and not producing SAM or responding haptotactically to SAM). These cells obey the CPM dynamics of Equations (1)–(4). When a cell in this state in the active zone senses a threshold local concentration of the activator (currently 0.75) it enters the condensing state, in which it produces SAM and starts responding haptotactically to SAM. The cell also starts to upregulate cell–cell adhesion (decreasing the parameter $J_{\text{cell,cell}}$ in the CPM from 7.0 to 0.5). A numerically determined mitosis doubling time (number of iterations required for the cell to reach twice the average size and divide) of 85 steps (for the zone growth rate mentioned above) gives the desired cell density of 64% throughout the simulation.

(2) Formation of skeletal pre-patterns of activating signal via RD PDEs (Section 2.2). We use the Schnakenberg equations following Murray (1993):

$$\begin{aligned} \frac{\partial u}{\partial t} &= \gamma(a - u + u^2 v) + \nabla^2 u, \\ \frac{\partial v}{\partial t} &= \gamma(b - u^2 v) + {}^{d}\nabla^2 v. \end{aligned} \tag{5}$$

Here, u is the activator concentration at location (x, y) and time t and v is the inhibitor concentration. γ is a parameter that affects the wavelength of the activator pattern.

We use a finite difference discretization in space with a forward Euler scheme for time. The domain moves in time, and we use no flux boundary conditions.

We choose solver parameters, $\Delta x = \Delta y = 0.01$, $\Delta t = 2E - 6$, to satisfy the standard stability criterion $d\Delta t / \min[(\Delta x)^2, (\Delta y)^2] < 1/4$. These parameters are independent of those in the CPM. The parameter $\gamma(y)$ controls the periodicity of the prepattern in the y direction.

(3) Cell differentiation using individual cell gene network ODEs and discrete rules (Section 2.3). Our limb simulation includes three types of cells: condensing, non-condensing and medium.

(4) Integration of submodels. We must integrate the submodels, particularly the stochastic CPM with continuum reaction–diffusion to allow the various mechanisms to work in a coordinated fashion:

(4.1) We match the spatial grid for continuum and stochastic models by interpolating the coarser spatial grid used in the explicit solution of the discretized reaction–diffusion equations to the discrete grid of the CPM. For example, in our simulation the RD domain is four times coarser than the domain for the CPM.

(4.2) We define the relative number of iterations for the RD and CPM evolvers. Diffusion, and hence establishment of the morphogen distributions, is rapid compared with growth for small domains. The time scales of these processes, however, become more comparable as outgrowth proceeds (cf. Dillon and Othmer, 1999, p. 310). Throughout, the domain for RD grows faster than that for CPM. The ratio of these growth rates is 1 : 1. We use a ratio of 50 iterations of RD for each CPM iteration.

(4.3) To control cell density in the active zone where cells divide and grow, we must balance the mitosis rate and the domain growth rate appropriately. We determined the parameters empirically.

4.2 Simulation results

Figure 2 shows a simulation of our model of limb formation. Cells cluster subject to haptotaxis and differential cell adhesion. The genetically governed response of cells to high activator concentration is to begin secreting SAM. Cells respond to SAM in two ways: (1) SAM causes cells to stick to the substrate; (2) SAM makes the cells more likely to condense by upregulating cell–cell adhesion. The activator concentration obeys the Schnakenberg RD equations (Section 3.2). An appropriate choice of control parameters gives the required pattern periodicity. The far right window shows the activator concentration; the pre-pattern directing the later cell condensation into the typical chondrogenic pattern is clear. The middle window represents the SAM concentration. Since cells exposed at some time to high activator concentration begin and continue to secrete SAM, and SAM in turn has the two effects described above, the SAM concentration pattern resembles the activator pre-pattern (Zeng *et al.*, 2003). Finally, the cells condense into the bone pattern of $1 + 2 + 3$ (where 3 corresponds to the three digits), shown in the left window.

The growth of the limb bud is not predefined. It depends on the cell division rate and how fast the cells can move. New cells generated by cell division push the limb tip upward. Thus growth occurs naturally. The computational domain corresponds to realistic values: 1.4 mm for the anteroposterior width; patterning begins at stage 20 of chicken embryo development. The proximo-distal dimension at stage 28 is 4 mm; about three times the width. A 100×300 grid covers the domain. This simulation ran in 93 min using a SunBlade 1000 with a 900 MHz CPU and 512 MB of memory.

5 DISCUSSION

The approach presented in this paper exploits the computational advantages of a continuum RD or simple diffusion formulation, while incorporating motion and advection of cells and of the viscous fluid medium through the CPM formalism. The detailed handling of cells and cellular dynamics allows fitting to more detailed biological and biophysical data.

This work has barely touched the modeling of the genetic regulatory network. Though CompuCell can model gene networks of any complexity, our sample simulations used a simplified model of cell differentiation.

Different constraints and limitations of our morphogenesis model are conceptual, model related or implementation related. The primary conceptual limitation is that relaxation to energy minima may not represent the biology. Limitations of the model are: (i) the model of growth is too simple, since it assumes that we know a priori the shape as a function of time: a model like that of Dillon and Othmer (1999) would be preferable; (ii) the CPM has many parameters; experiment can determine some but others require simulation tuning; (iii) RD is only one possible developmental pattern forming mechanism and simple diffusion or more complex genetic control may be more appropriate; and (iv) our model of cell differentiation comes from focused experimental studies to determine the key molecular components; extracting such knowledge from microarrays in a more automated way would complement these methods and increase their generality. Implementation related constraints are: (i) we do not include feedback from the cell on the PDE and (ii) we do not have an adaptive time step control for the relative speeds of growth and diffusion, which change during the simulation.

Despite these limitations, our model of limb development provides a framework which integrates a subcellular description of genetic regulation (in the form of ODEs and rules)

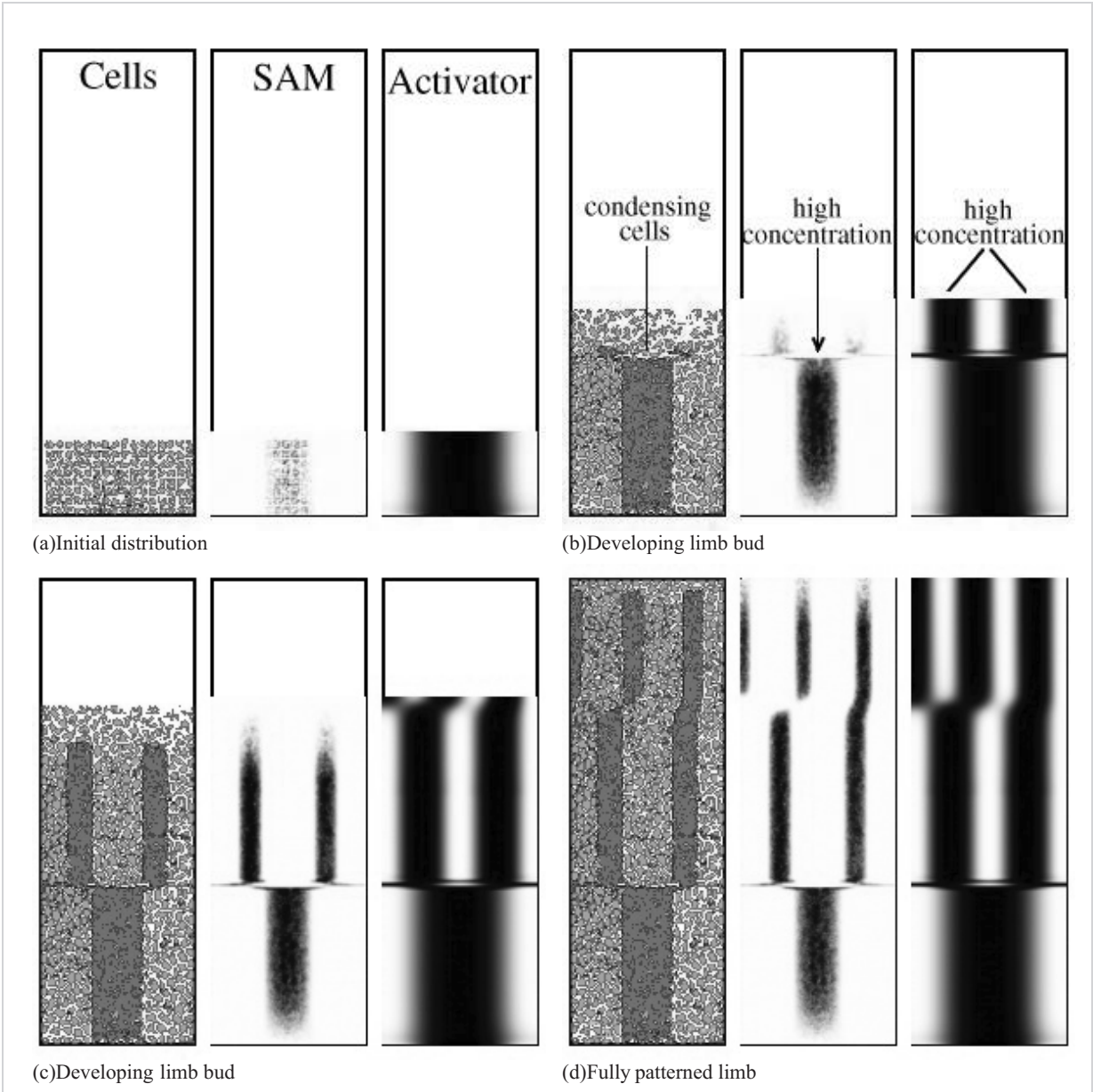

Fig. 2. Simulation of skeletal pattern formation in avian limb using CompuCell. For full limb, height to width ratio is 3 : 1. Figure not to scale (**a**) Initial distribution, (**b**) Developing limb bud, (**c**) Developing limb bud (**d**) Fully patterened limb.

with continuum and discrete models of spatial patterning and growth. The model allows fitting to experiments: (i) we can compare fate maps for cell tracking experiments and simulations; (ii) experiments measuring surface tensions in tissues can determine the contact energies in the CPM; (iii) we can compare gene expression experiments to the simulated gene expression; (iv) we can use experimental shapes as input to the model by providing a history of the domain over which we solve Equations (1)–(5), or we can compare experiments to models that attempt to produce the shapes themselves; and (v) we can compare experiments on chondrogenesis *in vitro* and *in vivo* to simulated patterns.

In our current extensions to this work, we are developing biologically authentic equations for the skeletogenesis example, extending the code to 3D, modeling of realistic geometries and including more detailed gene expression networks.

Related software developed by other groups includes Cytoscape (http://www.cytoscape.org/), which provides a framework to construct molecular interaction networks and

to integrate these networks with gene expression profiles and other state data; Virtual Cell (http://www.nrcam.uchc.edu/) models intracellular processes; Cello (http://mbi.dkfz-heidelberg.de/mbi/research/cellsim/cello/index.html) simulates tissues and cells; and E-Cell (http://ecell.sourceforge.net), which simulates cells and also has a powerful modeling, analysis and simulation environment. COMPUCELL provides modeling capabilities that are more comprehensive, and in many cases complementary to these programs.

ACKNOWLEDGEMENTS

This research was supported by an NSF Biocomplexity Grant No. IBN-0083653, NSF CAREER Award ACI-0135195, the Center for Applied Mathematics and the Interdisciplinary Center for the Study of Biocomplexity at the University of Notre Dame and the Biocomplexity Institute at Indiana University.

REFERENCES

Arkin,A.P., Ross,J. and McAdams,H.H. (1998) Nongenetic diversity: random gene expression mechanisms determine which phage lambda infected cells become lysogens. *Genetics*, **149**, 1633–1648.

Bowen,J., Hinchliffe,J.R., Horder,T.J. and Reeve,A.M.F. (1989) The fate map of the chick forelimb-bud and its bearing on hypothesized developmental control mechanisms. *Anat. Embryol.*, **179**, 269–283.

Chaturvedi,R., Izaguirre,J.A., Huang,C., Cickovski,T., Virtue,P., Thomas,G., Forgacs,G., Alber,M., Hentschel,G., Newman,S.A. and Glazier,J.A. (2003) Multi-model simulations of chicken-limb morphogenesis. In *Lecture Notes in Computational Science, LNCS 2659, Proceedings of the International Conference on Computational Science and Engineering ICCS 2003*, June 2003, Part III, pp. 39–49.

Dillon,R. and Othmer,H.G. (1999) A mathematical model for outgrowth and spatial patterning of the vertebrate limb bud. *J. Theor. Biol.*, **197**, 295–330.

Drury,J.L. and Dembo,M. (2001) Aspiration of human neutrophils: effects of shear thinning and cortical dissipation. *Biophys. J.*, **81**, 3166–3177.

Dudley,A.T., Ros,M.A. and Tabin,C.J. (2002) A re-examination of proximodistal patterning during vertebrate limb development. *Nature*, **418**, 539–544.

Frenz,D., Akiyama,S., Paulsen,D. and Newman,S. (1989a) Latex beads as probes of cell surface-extracellular matrix interactions during chondrogenesis: evidence for a role for amino-terminal heparin-binding domain of fibronectin. *Dev. Biol.*, **136**, 87–96.

Frenz,D.A., Jaikaria,N.S. and Newman,S.A. (1989b) The mechanism of precartilage mesenchymal condensation: a major role for interaction of the cell surface with the amino-terminal heparin-binding domain of fibronectin. *Dev. Biol.*, **136**, 97–103.

Gilbert,S.F. (1997) *Developmental Biology*, 5th edn. Sinauer Associates, Inc. Sunderland, MA.

Graner,F. and Glazier,J.A. (1992) Simulation of biological cell sorting using a two-dimensional extended Potts model. *Phys. Rev. Lett.*, **69**, 2013–2016.

Glazier,J.A. and Graner,F. (1993) A simulation of the differential adhesion driven rearrangement of biological cells. *Phys. Rev. E*, **47**, 2128–2154.

Held,L.I., Jr. (2002) *Imaginal Discs: The Genetic and Cellular Logic of Pattern Formation*. Cambridge University Press, New York.

Jong,H.D. (2002) Modeling and simulation of genetic regulatory systems: a literature review. *J. Comput. Biol.*, **9**, 67–103.

Lewis,J. (1975) Fate maps and the pattern of cell division: a calculation for the chick wing-bud. *J. Embryol. Exp. Morph.*, **33**, 419–434.

Leonard,C.M., Fuld,H.M., Frenz,D.A., Downie,S.A., Massague,J. and Newman,S.A. (1991) Role of transforming growth factor-beta in chondrogenic pattern formation in the embryonic limb: stimulation of mesenchymal condensation and fibronectin gene expression by exogenous TGF-beta and evidence for endogenous TGF-beta-like activity. *Dev. Biol.*, **145**, 99–109.

McAdams,H.H. and Arkin,A.P. (1999) Genetic regulation at the nanomolar scale: it's a noisy business!. *Trends Genet.*, **15**, 65–69.

Marée,F.M. and Hogeweg,P. (2001) How amoeboids self-organize into a fruiting body: multicellular coordination in *Dictyostelium discoideum*. *Proc. Natl Acad. Sci. USA*, **98**, 3879–3883.

Marée,F.M. (2000) From pattern formation to morphogenesis. Ph.D Thesis, Universiteit Utrecht.

Meinhardt,H. and Gierer,A. (2000) Pattern formation by local self-activation and lateral inhibition. *Bioessays*, **22**, 753–760.

Merks,R.M.H., Hoekstra,A.G., Kaandorp,J.A. and Sloot,P.M.A. (2003) Models of coral growth: Spontaneous branching, compactification and the Laplacian growth assumption. *J. Theor. Biol.*, **224**, 153–166.

Moftah,M.Z., Downie,S.A., Bronstein,N.B., Mezentseva,N., Pu,J., Maher,P.A. and Newman,S.A. (2002) Ectodermal FGFs induce perinodular inhibition of limb chondrogenesis *in vitro* and *in vivo* via FGF receptor 2. *Dev. Biol.*, **249**, 270–282.

Mombach,J., Glazier,J.A., Raphael,R. and Zajac,M. (1995) Quantitative comparison between differential adhesion models and cell sorting in the presence and absence of fluctuations. *Phys. Rev. Lett.*, **75**, 2244–2247.

Murray,J.D. (1993) *Mathematical Biology*, 2nd corrected edn (Biomathematics Vol. 19). Springer, Berlin, pp. 156, 376, 406, 472, 739.

Newman,S.A. (1988) Lineage and pattern in the developing vertebrate limb. *Trends Genet.*, **4**, 329–332.

Newman,S.A. and Comper,W. (1990) Generic physical mechanisms of morphogenesis and pattern formation. *Development*, **110**, 1–18.

Newman,S.A. and Frisch,H.L. (1979) Dynamics of skeletal pattern formation in developing chick limb. *Science*, **205**, 662–668.

Newman,S.A., Frisch,H.L. and Percus,J.K. (1988) On the stationary state analysis of reaction–diffusion mechanisms for biological pattern formation. *J. Theor. Biol.*, **134**, 183–197.

Oberlender,S. and Tuan,R. (1994) Expression and functional involvement of N-cadherin in embryonic limb chondrogenesis. *Development*, **120**, 177–187.

Page,K.M., Maini,P.K., Monk,N.A.M. and Stern,C.D. (2001) A model of primitive streak initiation in the chick embryo. *J. Theor. Biol.*, **208**, 419–438.

Steinberg,M.S. (1998) Goal-directedness in embryonic development. *Integrative Biol.*, **1**, 49–59.

Saunders,J.W.,Jr. (2002) Is the progress zone model a victim of progress? *Cell*, **110**, 541-543.

Turing,A. (1952) The chemical basis of morphogenesis. *Phil. Trans. R. Soc. London Ser. B*, **237**, 37–72.

Upadhyaya,A. (2000) Thermodynamic and fluid properties of cells, tissues and membranes. PhD Thesis, University of Notre Dame.

Wolpert,L. (2002) Limb patterning: reports of model's death exaggerated. *Curr. Biol.*, **12**, R628–R630.

Zeng,W., Thomas,G.L., Newman,S.A. and Glazier,J.A. (2003) A novel mechanism for mesenchymal condensation during limb chondrogenesis *in vitro*. In *Mathematical Modelling and Computing in Biology and Medicine, 5th ESMTB Conference 2002*. V. Società Editrice Esculapio, Bologna, pp. 80–86.